International Journal of Bifurcation and Chaos, Vol. 16, No. 7 (2006) 1989–1999


# DELAYED FEEDBACK SUPPRESSION OF COLLECTIVE RHYTHMIC ACTIVITY IN A NEURONAL ENSEMBLE

MICHAEL ROSENBLUM*, NATALIA TUKHLINA and ARKADY PIKOVSKY
*Department of Physics, University of Potsdam, PF 601553, D-14415 Potsdam, Germany*

LAURA CIMPONERIU
*Center for Research and Applications of Nonlinear Systems (CRANS), University of Patras, Greece*

Received November 5, 2004; Revised April 10, 2005

We analyze the delayed feedback approach to suppression of collective synchrony in a population of globally or randomly coupled neurons. In particular, we consider the main factors of imperfection of the control scheme and their influence on the suppression efficiency. Next, with the help of a realistic model of synaptically coupled population of inhibitory and excitatory neurons we demonstrate the potential of the suppression scheme for neurophysiological applications.

*Keywords*: Neuronal synchrony; delayed feedback control; global coupling; Rulkov model.

## 1. Introduction

Collective dynamics of large populations of neurons is widely studied in neurophysiological experiments as well as in theoretical works. These studies are motivated by the importance of macroscopic rhythmical activity in both physiological and pathological brain functioning. On the other hand, the understanding of cooperative behavior in a large ensemble of interacting units constitutes an important problem of nonlinear dynamics.

A particular problem of high practical importance is to develop techniques for the *control* of collective neuronal activity. The importance of this task is related to the hypothesis that pathological brain rhythms, e.g. observed in patients with Parkinson's disease and epilepsies, appear due to the synchrony of many thousands of neurons. Correspondingly, suppression of undesirable collective synchrony in a population of neurons is a challenging problem of neuroscience. Its solution may essentially improve the so-called *Deep Brain Stimulation* (*DBS*) technique, currently used in medical practice to suppress Parkinsonian and essential tremor [Benabid *et al.*, 1991]. This technique implies implantation of microelectrodes deep into the brain of a patient, either in the subthalamic nucleus or globus pallidus, and continuous stimulation of this target by a high frequency (about 100 or 120 Hz) periodic pulse train; the stimuli are delivered by a controller implanted into the chest. Noteworthy, in spite of rather broad usage of DBS[1] the neurophysiological mechanisms of such stimulation are poorly understood, and therefore its parameters are chosen by trial and error. Most likely, high

*URL: www.agnld.uni-potsdam.de/∼mros

[1]For example, one of the producers of DBS controllers, the Medtronic Inc, reports on over 20 thousands of patients using their devices.

frequency DBS mimics lesioning of the tissue by quenching the firing of neurons. This fact, as well as the necessity to apply the (rather strong) stimulation continuously, calls for development of more efficient suppression techniques.

Development of model based DBS techniques exploiting the methods of nonlinear dynamics and statistical physics was pioneered by P. A. Tass, who proposed a number of approaches. The main idea of these approaches is that suppression of the pathological rhythm should be achieved in such a way that (i) activity of individual units is not suppressed, but only their firing becomes asynchronous, and (ii) the stimulation should be minimized, e.g. it is desirable to switch it off as soon as the synchrony is suppressed (see [Tass, 1999, 2001, 2002a, 2002b, 2002c, 2002d, 2003] and references therein). Following these ideas we suggested in our previous publications [Rosenblum & Pikovsky, 2004a, 2004b] a delayed feedback suppression control scheme (Fig. 1) which we further analyze in this paper. In our approach it is assumed that the collective activity of many neurons is reflected in the local field potential (LFP) which can be registered by an extracellular microelectrode. The delayed and amplified LFP signal can be fed back into the system via the second or same electrode (see [Ozden *et al.*, 2004] and references therein for a description of one electrode measurement-stimulation setup). Numerical simulation as well as analytical analysis of the delayed feedback control demonstrate that it indeed can be exploited for suppression of the collective synchrony.

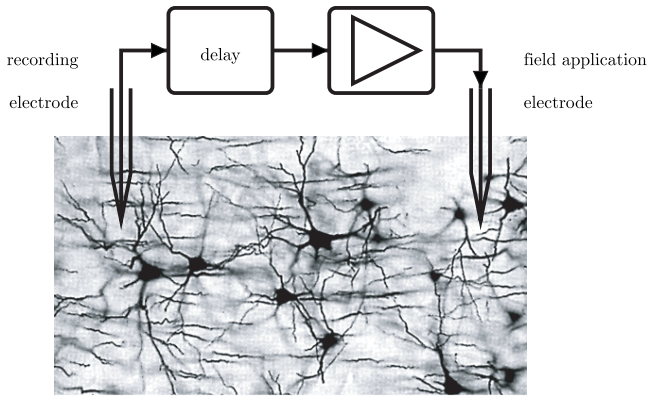


Fig. 1. Scheme of the suggested approach to deep brain stimulation [Rosenblum & Pikovsky, 2004a, 2004b]. The local electrical field in a neuronal population should be measured by the recording electrode and fed back via the field application electrode. The device should contain a delay line and an amplifier.

Mechanisms of generation of Parkinsonian tremor are not yet completely understood. In spite of attempts to develop detailed mathematical description of oscillatory processes in corresponding parts of the brain, i.e. in subtalamic nucleus and external global pallidius networks (see [Bevan *et al.*, 2002; Rubin & Terman, 2004] and references therein), there is no well-accepted model that can be exploited as a test system for simulation of DBS. Besides, such modeling would require very high computational resources. Correspondingly, the DBS techniques based on the ideas of nonlinear dynamics have been so far tested only on a relatively simple conceptual models: globally coupled phase [Tass, 1999, 2001, 2002a, 2002b, 2002c, 2002d, 2003] or neuronal [Rosenblum & Pikovsky, 2004a, 2004b] oscillators. Thus, only suppression of activity of an isolated neuronal population has been considered so far. In the present paper we further elaborate on this important problem and mostly remain within this framework. However, we make several steps towards mode realistic modeling, in particular we consider more realistic coupling between neuronal units via synaptic connections. Next, there are many issues, important for the practical applications, like influence of measuremental noise, finite-size effects, or impact of the connectivity in the network, which can hardly be treated analytically or have not been considered in the idealized model studied in [Rosenblum & Pikovsky, 2004a, 2004b]. These issues are also addressed in the present paper.

## 2. Suppression of Synchrony in Ensemble of Globally Coupled Neurons

### 2.1. *Phenomenological description and minimal model*

Theoretical analysis of the delay controlled ensemble dynamics is related to the assumption that emergence of collective synchrony can be understood as the Kuramoto transition [Kuramoto, 1975, 1984; Winfree, 1980; Mirollo & Strogatz, 1990] Analytical treatment of the problem can be performed only for an idealized model under assumption of (i) global (each-to-each) interaction, (ii) infinitely large ensemble size, and (iii) weak coupling (i.e. in the phase approximation) [Rosenblum & Pikovsky, 2004a]. Another approach is based on a quite general consideration of the Kuramoto synchronization

transition in an ensemble as the Hopf bifurcation for the mean field, and on the analysis of the corresponding model amplitude equation (normal form) for the dynamics of the complex mean field $A$ [Kuramoto, 1984; Crawford, 1994]. With the account of a delayed feedback loop, this equation takes the form [Rosenblum & Pikovsky, 2004b]

$$\dot{A} = (\varepsilon - \varepsilon_{cr} + i\omega)A + \varepsilon_f e^{-i\alpha}\mathcal{L}(A(t), A(t-\tau)) - \zeta|A|^2 A. \quad (1)$$

Here the factor $\varepsilon$ describes the internal global coupling in the ensemble; if it exceeds the critical value $\varepsilon_{cr}$ then synchrony sets in the population and macroscopic mean field appears. $\varepsilon_f$ describes the strength of the feedback and $\tau$ is the delay; the phase shift $\alpha$ depends on the properties of individual oscillators and on how the feedback term appears in their equations. The operator $\mathcal{L}$ has different form for different feedback schemes, discussed and compared below. Qualitatively, the effect of the delayed feedback can be understood in the following way: for proper feedback parameters $\varepsilon_f, \tau$ the delayed term compensates the instability due to internal coupling (described by increment $\varepsilon - \varepsilon_{cr}$) and thus changes the linear stability of the system.

Theoretical analysis of Eq. (1) provides the domains of control, i.e. the ranges of delay time and amplification in the feedback loop for which the control is effective. These results are in a good correspondence with the numerical simulation of the ensemble dynamics with different neuron models used for the description of individual units (Bonhoefer–van der Pol or Hindmarsh–Rose equations [Hindmarsh & Rose, 1984], Rulkov map model [Rulkov, 2001]), see [Rosenblum & Pikovsky, 2004b]. We illustrate this using a computationally efficient neuronal model, proposed by Rulkov [2001, 2002] and further developed in [Rulkov *et al.*, 2004]. In this model a neuron is described by a 2D map. In spite of its simplicity, this model reproduces most regimes exhibited by the full Hodgkin–Huxley model, but at essentially lower computational costs, thus allowing detailed analysis of the dynamics of large ensembles. In Fig. 2 we demonstrate the results of the simulation of delayed feedback suppression in an ensemble of Rulkov neurons

$$\begin{aligned} x_i(n+1) &= \frac{4.3}{1+x_i^2(n)} + y_i(n) + \varepsilon X(n) + \mathcal{C}, \\ y_i(n+1) &= y_i(n) - 0.01(x_i(n)+1), \end{aligned} \quad (2)$$

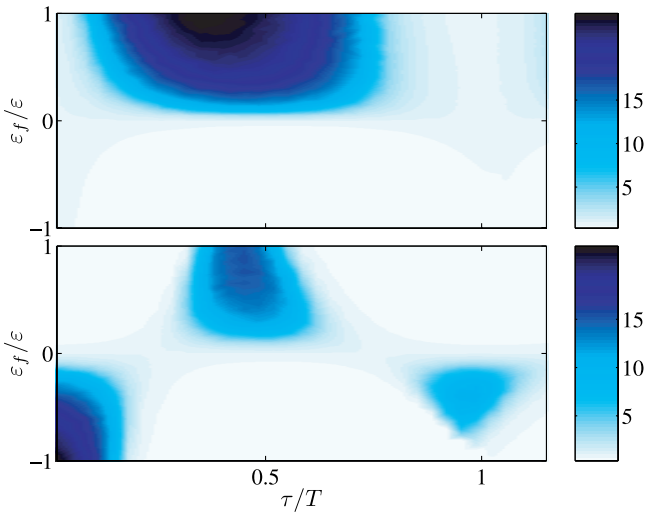


Fig. 2. Domains of control for the system (2) in the parameter plane delay — feedback strength, for differential (top panel) and direct (bottom panel) schemes. Color codes the coefficient of suppression (see text). Internal coupling is $\varepsilon = 0.06$.

where $n$ is the discrete time, $i = 1, \ldots, N$ is the index of a neuron in the population, and

$$X(n) = \frac{1}{N}\sum_{1}^{N} x_i(n)$$

is the mean field. The delayed-feedback control is described by the term $\mathcal{C}$. In the following we consider two types of feedback: direct control $\mathcal{C} = \varepsilon_f X(t-\tau)$ and differential control $\mathcal{C} = \varepsilon_f(X(t-\tau) - X(t))$. The parameters in Eqs. (2) are chosen in such a way that individual units are in the regime of chaotic bursting. The efficiency of suppression is quantified by the suppression factor

$$S = \left(\frac{\mathrm{var}(X_{\mathrm{off}})}{\mathrm{var}(X_{\mathrm{on}})}\right)^{1/2}, \quad (3)$$

where $X_{\mathrm{off}}$ and $X_{\mathrm{on}}$ are the mean fields observed in the case of the feedback off or on, respectively. High values of $S = S(\tau, \varepsilon_f)$ (Fig. 2) provide the domains of control. Certainly, the suppression in the system (2) is not perfect: the suppression factor remains finite due to finite-size effects, discussed below. In other words, the suppressed mean field is not zero, but exhibits some irregular fluctuations due to a finite number of the elements in the ensemble. Correspondingly, the borders of the control domains can be determined only approximately, by setting some cut-off level. However, the shape and position of domains of control are in a good correspondence with the results of the theoretical analysis of Eq. (1),

which describes the idealized case of infinitely large population size. Figure 2 demonstrates that suppression of the synchrony can be achieved both by the direct and differential control schemes. This example also shows that differential control provides less domains of control, but these domains are generally larger and the suppression factor is higher. Another advantage of the differential control scheme is that it provides noninvasive suppression, in the sense that $\lim_{N\to 0} \mathcal{C} = 0$, whereas for the direct control suppression is generally invasive, $\lim_{N\to 0} \mathcal{C} = \text{const}$.

## 2.2. *Realistic model of a synaptically coupled ensemble*

In this section we go beyond the minimal model (2) and explore the possibility of population rhythms suppression in a physiologically plausible model of a neuronal ensemble. For this purpose, we use, following [Rulkov *et al.*, 2004], a model of rhythmic activity in a neuronal population of excitatory and inhibitory neurons with intrinsic properties and connectivity structure reminiscent of real neuronal networks.

*Excitatory neurons* are modeled as regular spiking (RS) neurons, which are the most typical neurons in the cortex. They are characterized by repetitive firing in response to a depolarizing input current and an intrinsic spike-frequency adaptation mechanism, i.e. their firing rate slows down during a prolonged depolarizing current. *Inhibitory neurons* are of fast spiking (FS) type, that is, they show little or no adaptation when compared with regular spiking (RS) neurons. Both types of neurons are described by a phenomenological map-based model of spiking-bursting neuronal activity [Rulkov, 2001, 2002; Rulkov *et al.*, 2004], which reproduces the typical firing patterns displayed by cortical neurons, such as regular spiking, fast spiking, and intrinsic bursting.

Each inhibitory neuron is modeled by

$$x(n+1) = f(x(n), x(n-1), y_{\text{rs}} + \beta(n)), \qquad (4)$$

where $n$ is the discrete time, $y_{\text{rs}}$ is constant rest potential, and the nonlinear function $f(\cdot)$ is given by

$$f(x(n), x(n-1), u(n)) = \begin{cases} \dfrac{\alpha}{1-x(n)} + u(n) & \text{if } x(n) \le 0, \\ \alpha + u(n) & \text{if } x(n) < \alpha + u(n) \ \text{ and } \ x(n-1) \le 0, \\ -1 & \text{if } x(n) \ge \alpha + u(n) \ \text{ and } \ x(n-1) > 0, \end{cases} \qquad (5)$$

where $u(n) = y_{\text{rs}} + \beta(n)$, and $\alpha$ is a parameter. Variable $\beta(n)$ incorporates the action of (total) synaptic $I_{\text{syn}}$ and nonsynaptic $I_{\text{ext}}$ input currents entering the neuron:

$$\beta(n) = \beta_{\text{syn}} I_{\text{syn}}(n) + \beta_{\text{ext}} I_{\text{ext}}(n) + \beta_{\text{hp}} I_{\text{hp}}, \qquad (6)$$

where $\beta_{\text{syn}}$, $\beta_{\text{ext}}$, and $\beta_{\text{hp}}$ are constants. $I_{\text{hp}}$ is an intrinsic hyperpolarizing current which dynamics is described by

$$I_{\text{hp}}(n+1) = \begin{cases} \gamma_{\text{hp}} I_{\text{hp}}(n) - g_{\text{hp}} & \text{if neuron fires,} \\ \gamma_{\text{hp}} I_{\text{hp}}(n) & \text{otherwise} \end{cases} \qquad (7)$$

where $g_{\text{hp}}$ and $\gamma_{\text{hp}}$ are constants. (Here the condition of firing at time $n$ is equivalent to the condition $x(n) < \alpha + u(n)$ and $x(n-1) \le 0$, cf. Eq. (5).)

Excitatory neurons are modeled by two-dimensional maps, which allow to describe the mechanism of firing rate adaptation. The model has the form:

$$\begin{aligned} x(n+1) &= f(x(n), x(n-1), y(n) + \beta(n)), \\ y(n+1) &= y(n) - \mu(x(n) + 1) + \mu\sigma_1 + \mu\sigma(n), \end{aligned} \qquad (8)$$

where $x(n)$ and $y(n)$ are the fast and the slow dynamical variables, respectively, $0 < \mu \ll 1$ and $\sigma_1$ are parameters, and $f(\cdot)$ is given by Eq. (5). Action of input currents is described by variables $\beta(n)$ and $\sigma(n)$:

$$\begin{aligned} \beta(n) &= \beta_{\text{syn}} I_{\text{syn}}(n) + \beta_{\text{ext}} I_{\text{ext}}(n), \\ \sigma(n) &= \sigma_{\text{syn}} I_{\text{syn}}(n) + \sigma_{\text{ext}} I_{\text{ext}}(n). \end{aligned} \qquad (9)$$

While modeling a population of neurons, we use Eqs. (4)–(9) to describe the dynamics of each neuron, labeling corresponding variables by an upper index $i = 1, \ldots, N$.

*Synaptic connections* between neurons are characterized by their own, quite complicated, dynamics. If there is a synaptic connection from $j$th neuron to $i$th neuron, then, whenever the neuron

with index $j$ fires, it produces a current in the neuron $i$; we denote this current as $I_{\rm syn}^{(i\leftarrow j)}$. The $i$th and $j$th neurons are called postsynaptic and presynaptic neurons, respectively. The total normalized synaptic current received by $i$th neuron is given by the normalized sum of synaptic currents from all neurons which have connections targeting the given neuron, i.e.

$$I_{\rm syn}^{(i)}(n) = N_e^{-1} \sum_{\rm (exc)} I_{\rm syn}^{(i\leftarrow k)}(n) + N_i^{-1} \sum_{\rm (inh)} I_{\rm syn}^{(i\leftarrow l)}(n), \tag{10}$$

where $N_e$ and $N_i$ are the number of excitatory and inhibitory neurons, respectively, and the first (second) sum is taken over all excitatory (inhibitory) neurons, targeting the $i$th neuron. Normalization by $N_e$ and $N_i$ is performed in order to keep the balance between excitation and inhibition for different sizes of the ensemble, so that the size effects are avoided. The time course of a postsynaptic current is given by:

$$I_{\rm syn}(n+1) = \begin{cases} \gamma I_{\rm syn}(n) - d(n) g_{\rm syn}(x_{\rm post}(n) - x_{\rm rp}) & \\ & \text{if } x_{\rm pre}(n) \text{ fires,} \\ \gamma I_{\rm syn}(n) & \text{otherwise,} \end{cases} \tag{11}$$

where parameter $\gamma$ defines the decay rate of the synaptic current, $g_{\rm syn}$ is the maximum strength of synaptic coupling, and $x_{\rm rp}$ denotes the reversal potential of the synapse,[2] condition "$x_{\rm pre}(n)$ fires" means firing of the presynaptic neuron at the time $n$. The indices *pre* and *post* stand for the presynaptic and postsynaptic variables, respectively. Variable $d(n)$ models a neurochemical mechanism of synaptic plasticity called synaptic depression, which is associated with a decrease of the synaptic strength in response to successive firing of the presynaptic neuron. For excitatory synapses between RS neurons, the time course of synaptic depression is modeled by

$$d(n+1) = \begin{cases} (1-d_{\rm dep}) d(n) & \text{if } x_{\rm pre}(n) \text{ fires,} \\ 1 - (1-d_{\rm rec})(1-d(n)) & \text{otherwise,} \end{cases} \tag{12}$$

where $d_{\rm dep}$ and $d_{\rm rec}$ are parameters. For other synaptic connections, the plasticity is neglected and $d(n)$ is assumed to be constant, $d(n) = 1$.

*Suppression of the collective rhythm* in an ensemble of excitatory and inhibitory neurons was simulated with the help of the model of $N_e = 1000$ excitatory RS neurons and $N_i = 200$ inhibitory FS neurons. The connectivity is assumed to be all-to all, with excluded self-connections. For simplicity, we neglect the synaptic transmission delays. Firing-rate heterogeneity within the ensemble is ensured by external currents $I_{\rm ext}^{(i)}$, where $i$ is the index of a neuron; these currents model the influence of distant brain areas. In our simulation, we take $I_{\rm ext}^{(i)} = \text{const}$ for each neuron, but randomly distributed across the ensemble. We choose a Gaussian distribution centered at 0.05 with $\text{rms}(I_{\rm ext}^{(i)}) = 0.01$, which results in individual firing rates of RS and FS neurons centered around $\approx 11\,$Hz and $\approx 30\,$Hz, respectively (see Fig. 3). The parameters for the simulation has been taken from [Rulkov *et al.*, 2004]. The parameter set for RS neurons is: $\mu = 0.0005$, $\alpha = 3.65$, $\sigma_1 = 0.006$, $\sigma_{\rm syn} = \sigma_{\rm ext} = 1$, $\beta_{\rm syn} = \beta_{\rm ext} = 0.133$, $y_{\rm rs} = -2.9$. The parameter set for FS neurons is: $\mu = 0.002$, $\alpha = 3.8$, $\sigma_{\rm syn} = \sigma_{\rm ext} = 1$, $\gamma_{\rm hp} = 0.6$, $\beta_{\rm syn} = \beta_{\rm ext} = 0.1$, $g_{\rm hp} = 0.3$, $\beta_{\rm hp} = 0.5$. Parameters of synaptic connections are: $\gamma = 0.6$, $x_{\rm rp} = 0$ for excitatory and $\gamma = 0.8$, $x_{\rm rp} = -1.1$ for inhibitory synapses, $d_{\rm dep} = 0.5$ and $d_{\rm rec} = 0.01$.[3]

With the increase of the synaptic coupling between the neurons, the model demonstrates a transition from independent firing to coherent collective activity. A detailed analysis of the emergence of rhythmic activity in the ensemble and its dependence on intrinsic neuronal dynamics, properties of synaptic coupling and connectivity is outside the framework of the present study. Here we briefly describe the pattern of rhythmical activity and the effect of the feedback, displayed by the ensemble considered here. Collective rhythm of the uncontrolled system example of the output for an oscillatory state is displayed in the middle column of Fig. 3. It can be seen, that under the condition of a relatively strong excitation ($g_{{\rm syn},RS\to RS} = 2.2$, $g_{{\rm syn},RS\to FS} = 1.0$, $g_{{\rm syn},FS\to FS} = g_{{\rm syn},FS\to RS} = 0.2$), the ensemble generates stable macroscopic oscillations consisting of bursts of high frequency activity repeated at a low rate $\approx 6\,$Hz. It is

[2]The reversal potential is the voltage at which the postsynaptic effect reverses sign.

[3]The choice of parameters is motivated by the dynamics of excitatory synapses involving the $AMPA$ receptors and inhibitory synapses involving $GABA_A$ receptors. Note the larger relaxation time of inhibition compared to excitation.

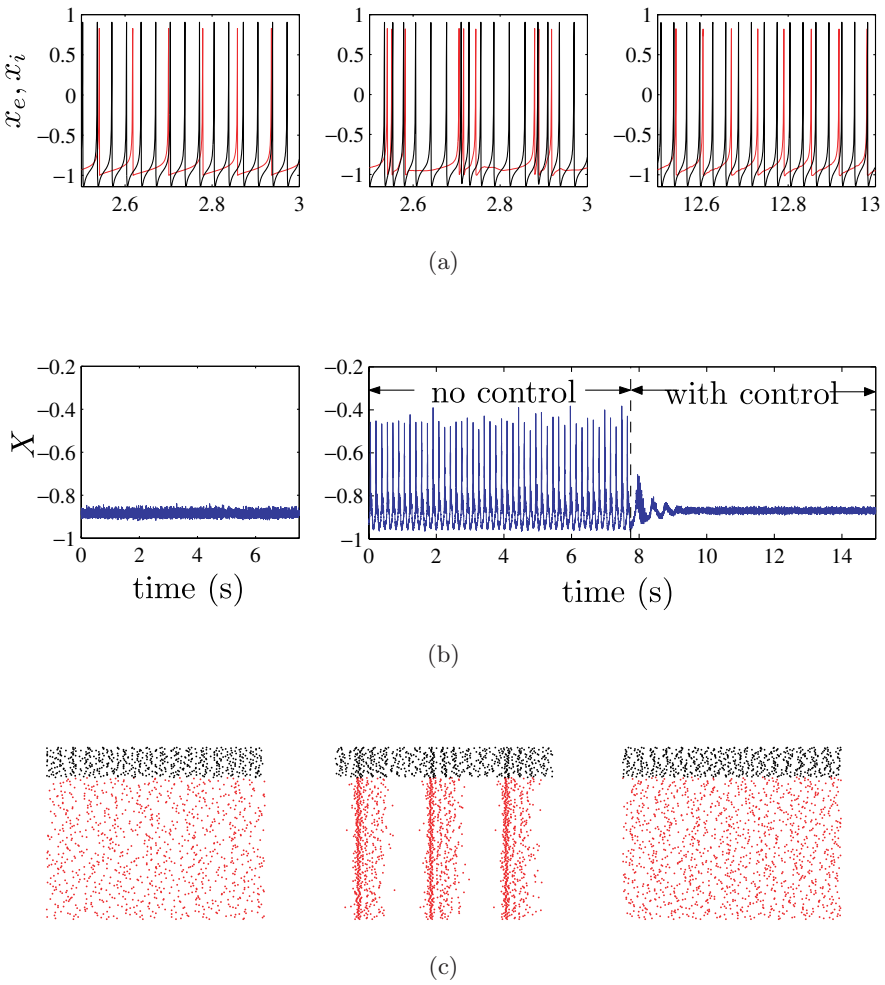


Fig. 3. Suppression of collective neuronal activity in an heterogenous ensemble of excitatory/inhibitory neurons. (a) Activity of one excitatory (red) and one inhibitory (black) neuron, for the uncoupled neurons (left), coupled neurons (middle), and coupled neurons in the presence of delayed feedback (right panel). Respectively, (b) and (c) show for the same conditions the ensemble mean field activity $X$ and raster plots of the firing times of all neurons within the ensemble over the 0.05 s time interval.

important to note that bursting is an ensemble effect of RS excitatory neurons, because isolated neurons fire regularly. This is consistent with the previous study which has shown that a major determinant of synchronized burst activity in networks of excitatory regularly spiking neurons is the spike-frequency adaptation mechanism [van Vreeswijk & Hansel, 2001].

In modeling suppression of population rhythm in an ensemble of RS–FS neurons we assume that the control input acts as a common for all neurons input current

$$I_f(n) = \varepsilon_f(X(n-\tau) - X(n)), \qquad (13)$$

where $X(n) = 1/N \sum_i x_i(n)$ is the ensemble mean field. We treat $I_f(n)$ as an additional external current which enters the r.h.s of Eqs. (6) and (9), so that the correspondent term becomes $\beta_{\text{ext}}(I_{\text{ext}}+I_f)$. The control parameters $\varepsilon_f$ and delay $\tau$ determine the efficacy of the suppression control. In the right panel of Fig. 3 we illustrate efficient suppression of the collective rhythm for the parameter values $\varepsilon_f = 0.8$ and $\tau = 0.035s \approx T/4$.

## 3. Beyond Idealized Model

### 3.1. *Global coupling versus random coupling*

Global coupling in an ensemble is a theoretically convenient approximation. Here we numerically explore how good this approximation works, if the

neurons are in fact coupled in a more complex, random, way. There are many possibilities to model a randomly coupled network. We consider that each of $N = 10000$ neurons has $N_l$ links, i.e. it is coupled to $N_l$ randomly chosen elements of the population. The coupling strength $\varepsilon$ within each pair is taken to be the same. In Fig. 4 we plot the dependence of the variance of the mean field $\mathrm{var}(x)$ on $\varepsilon$ for different number of links $N_l$. The synchronization transition is similar to the case of the global coupling, though it takes place for higher values of $\varepsilon$. We see that the bifurcation curve for $N_l = 50$ practically coincides with that for the global coupling case. Thus, the dynamics of an ensemble with random coupling to $N_l$ neighbors is qualitatively close to the dynamics of the globally coupled population. The delayed feedback control (direct scheme with $\tau = 30$ was used here) shifts the bifurcation curves (Fig. 5), thus allowing one to control the transition, as in case of global coupling.[4] Indeed, a shift of the bifurcation curve to the right means decrease of the mean field variance for given value of the internal coupling in the ensemble, thus providing suppression up to the level of noise fluctuations in the system if the bifurcation value becomes larger than the internal coupling. This is supported by the computation of the control domains (the results are similar to those shown in Fig. 2 and therefore are not given here).

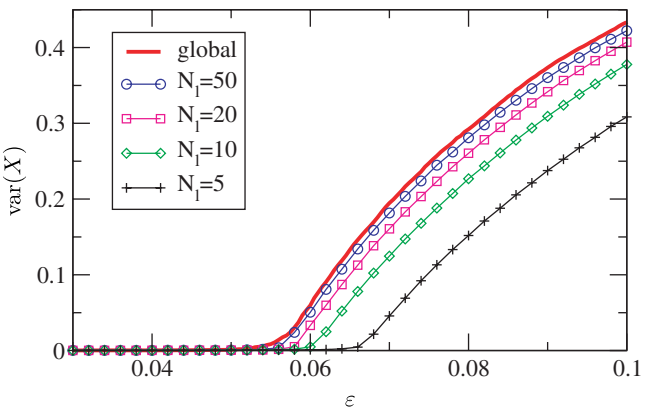


Fig. 4. Comparison of synchronization transition in ensembles with all-to-all coupling and random coupling, when each unit is coupled to $N_l$ units. Bold red line shows the transition for the case of all-to-all coupling. It is seen that the dynamics of the ensemble with global coupling is very close to the case of an ensemble with $N_l = 50$. For smaller number of links, the dynamics is qualitatively similar, though the synchronization transition happens for larger coupling $\varepsilon$.

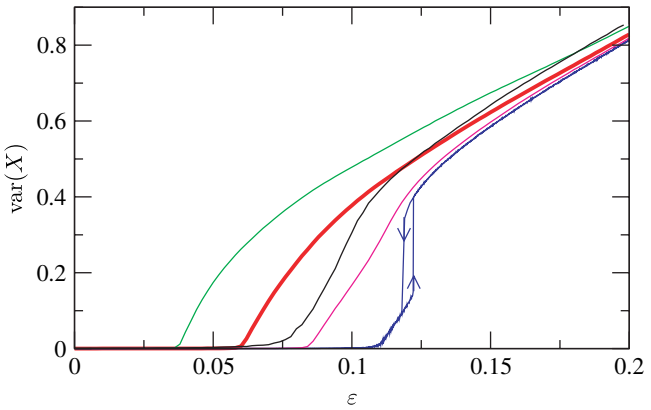


Fig. 5. Control of a randomly coupled ensemble of Rulkov neurons, $N_l = 10$. Red curve illustrates the transition in the uncontrolled system. Green, magenta, and blue curves correspond to the case when the mean field of the whole population has been used for the control, with the feedback strength $\varepsilon_f = -0.02$, $\varepsilon_f = 0.02$, and $\varepsilon_f = 0.04$, respectively. The black curve corresponds to the feedback with the local field measured at a randomly chosen site, $\varepsilon_f = 0.02$; this field is computed as an average over the $N_l = 10$ units coupled to this site.

Black curve in Fig. 5 illustrates the case when the feedback signal is not the mean field of the whole population but the local field, acting on one neuron. It is, $\mathcal{C} = \varepsilon_f N_l^{-1} \sum_l x_l$, where index $l = 1, \ldots, N_l$ numerates the neurons linked to the chosen one. This example, to be compared with that illustrated in Fig. 7 below, demonstrates that such an imperfect measurement however provides suppression, though it is not so effective as the control via mean field $X$ (red curve). Summarizing the results presented in Fig. 5, we conclude that mean field approximation works very well even for moderate connectivity of the network (50 links in an network of 10000 elements in our example).

Note that for a certain parameter choice (negative $\varepsilon_f$ for the given delay $\tau = 30$) the bifurcation curves are shifted to the left, which means that collective synchrony can be enhanced. This property of the feedback control complicates the adjustment of parameters for suppression, but, on the other hand, makes this technique suitable for excitation of collective oscillations. The latter feature might be used, e.g. in studies with experimental (brain slice) models of Parkinson's disease and epilepsy.

[4]Note that sufficiently strong feedback, $\varepsilon_f = 0.04$, changes the type of the bifurcation; now the transition exhibits hysteresis, see blue curve in Fig. 5. See also a discussion in [Rosenblum & Pikovsky, 2004a].

### 3.2. *Finite size effect and imperfection of the feedback loop*

In this section we numerically analyze the factors that we cannot take into account in our analytical treatment. Having demonstrated that the mean field (all-to-all) approximation provides nearly the same results as the random coupling, in the following we remain in the framework of the globally coupled ensemble, because of high computational efficiency of this model. We analyze the factors which make both this model and the control loop nonideal. Namely, we simulate the influence of the finite ensemble size, effect of noise in the measurements, etc. In our computations we use 10000 Rulkov neurons and keep the internal coupling in the Rulkov ensemble $\varepsilon = 0.06$.

#### 3.2.1. *Finite size effects*

Numerical analysis shows that the dependence of the suppression factor on the population size $N$ can be perfectly fit by the square root function, $S \sim \sqrt{N}$, in correspondence to theoretical considerations. Indeed, in the finite-size population the mean field below the synchronization threshold can be treated as a noise with the variance $\sim N^{-1}$ [Pikovsky & Ruffo, 1999]. On the other hand, for $\varepsilon > \varepsilon_{\rm cr}$, $\mathrm{var}(X)$ does not practically depend on $N$ and, at least for small subcriticality, $\mathrm{var}(X) \sim \sqrt{\varepsilon - \varepsilon_{\rm cr}}$ (provided the Hopf bifurcation for the mean field is the supercritical one). Hence, the maximal possible suppression $S \sim \sqrt{(\varepsilon - \varepsilon_{\rm cr})N}$.

#### 3.2.2. *Additive noise in measurements*

We model the situation when the mean field is measured with an error, so that the stored signal is $X_\tau = X(t-\tau) + \xi$, where $\xi$ is taken as white Gaussian noise. Simulations show that the suppression technique is quite robust with respect to measuremental noise: if $\mathrm{rms}(\xi)/\mathrm{rms}(X) \approx 0.5$ the suppression is still rather high, $S \approx 5$, see Fig. 6.

#### 3.2.3. *Imperfect mean field measurement*

Now we suppose that the recording electrode measures not the mean field of the whole ensemble, but the mean field of a subpopulation containing $qN$ neurons, $q \le 1$, i.e. the control term has the form $\varepsilon_f X_q(t-\tau)$, where $X_q = (qN)^{-1}\sum_1^{qN} x(j)$, and $j = 1, \ldots, qN$ are the indices of a (randomly) picked subpopulation. Using $X_q$ as the feedback signal still allows one to control the synchrony in the ensemble, and the impact of the parameter $q$ turns out to be similar to the finite-size effect (Fig. 7); here $\tau = 30$, $\varepsilon_f/\varepsilon = 1$.

#### 3.2.4. *Imperfect action*

Here we suppose that the radiated signal acts only on a subpopulation of the size $qN$, $q \le 1$. Simulations show that this imperfect action is equivalent to a decrease of feedback factor $\varepsilon_f$, see Fig. 8. Here we show two curves: the first one (boxes) corresponds to variation of $\varepsilon_f$ from zero to $\varepsilon_f^{\max} = 1.5$, whereas the second one (circles) corresponds to variation

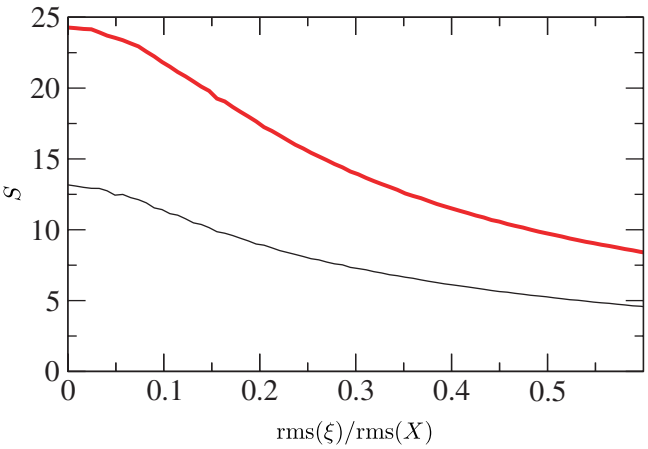


Fig. 6. Suppression coefficient versus intensity of additive noise in the measurement, for differential (red) and direct (black) schemes, $\varepsilon = \varepsilon_f = 0.06$, $\tau = 30$. For the presentation, the noise is normalized by the root mean square of the mean field in the uncontrolled ensemble.

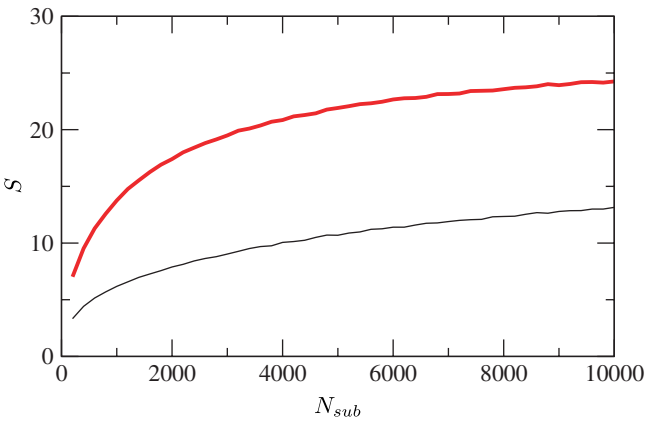


Fig. 7. Efficiency of the control for the fixed population size $N = 10000$, for differential (red) and direct (black) schemes, in dependency on the size of the subpopulation $N_{\rm sub} = qN$, where the mean field is registered (see text).

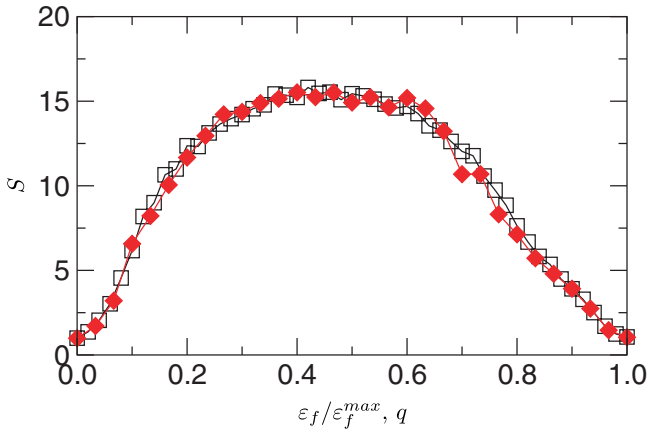


Fig. 8. Efficiency of the control in case when only a subpopulation of the size $qN$ is affected by the feedback field for the constant feedback factor $\varepsilon_f = \varepsilon_f^{\max} = 1.5$ (black boxes). This curve should be compared with another one for the case when the whole population is affected ($q = 1$), but the feedback factor is varied from zero to $\varepsilon_f^{\max}$ (red diamonds). Overlap of two curves demonstrates that imperfect stimulation, i.e. an action on a subpopulation is equivalent to decrease of the feedback strength $\varepsilon_f$.

of the subpopulation size $qN$. One can see that the dependence of $S$ on $q$ can be not monotonic, what corresponds to crossing a domain of control, cf. Fig. 2

Similar dependence is observed for the differential scheme. Thus, action on a subpopulation is equivalent to decrease of the feedback strength, and therefore can be compensated, unless $q$ becomes very small. We illustrate this with Fig. 9, where we show the dependence of the suppression

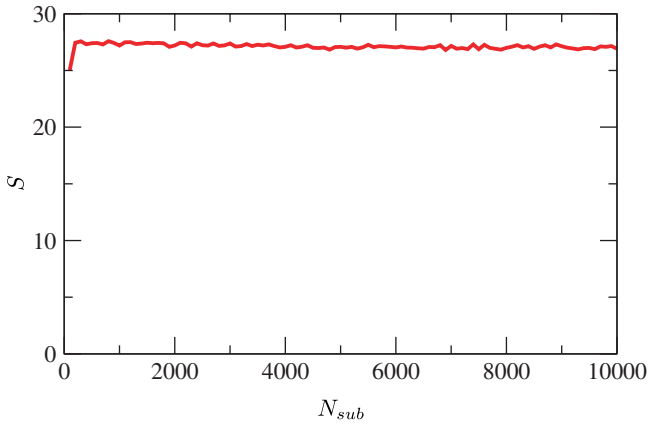


Fig. 9. Imperfect stimulation: delayed signal acts on the subpopulation of size $N_{\rm sub} = qN$. This imperfection can be compensated by increasing the feedback strength, $\varepsilon_f \sim 1/\sqrt{N_{\rm sub}}$. As a result, the suppression factor can be kept constant unless $N_{\rm sub}$ becomes very small, $N_{\rm sub} \approx 200$; differential control scheme is used in this example.

factor on the size of the population, influenced by the feedback. Here the feedback strength was kept according to $\varepsilon_f/\varepsilon = 2/q$.

Of special interest is the case when two electrodes record and stimulate the activity of two different, though overlapping populations. This situation is treated in the next section.

## 4. Case of Two Interacting Neuronal Ensembles

For the following it is convenient to consider the population of neurons, generating the undesired rhythm, as consisting of two subpopulations: first one is affected by the stimulating electrode, and the mean field of the second one is measured by the recording electrode. For simplicity we assume that these populations do not overlap. In the spirit of a phenomenological description outlined in Sec. 2.1, we, instead of using Eq. (1), describe the population by two symmetrically coupled equations for the complex amplitudes $A$, $B$:

$$\begin{aligned}\dot{A} &= (\xi_1 + i\omega_1)A - |A|^2 A + \varepsilon(B - A) \\ &\quad + \varepsilon_f B(t - \tau), \\ \dot{B} &= (\xi_2 + i\omega_2)B - |B|^2 B + \varepsilon(A - B).\end{aligned} \tag{14}$$

For generality, we first admit different parameters (frequencies and increments) for both systems. To analyze the stability, we substitute in (14) $A = e^{\lambda t}$, $B = ke^{\lambda t}$, where $k$ is complex, and, considering only linear terms, obtain the system of characteristic equations

$$\begin{aligned}\lambda &= (\xi_1 + i\omega_1) + \varepsilon(k - 1) + \varepsilon_f k e^{-\lambda\tau}, \\ k\lambda &= k(\xi_2 + i\omega_2) + \varepsilon(1 - k).\end{aligned} \tag{15}$$

Excluding $k$ we get:

$$(\lambda + \varepsilon - \xi_1 - i\omega_1)(\lambda + \varepsilon - \xi_2 - i\omega_2) = \varepsilon^2 + \varepsilon\varepsilon_f e^{-\lambda\tau}. \tag{16}$$

Taking $\lambda = i\nu/\tau$ on the stability border and writing the real and imaginary parts, we get:

$$\begin{aligned}&(\xi_1 - \varepsilon)(\xi_2 - \varepsilon) - \left(\omega_1 - \frac{\nu}{\tau}\right)\left(\omega_2 - \frac{\nu}{\tau}\right) - \varepsilon^2 \\ &\qquad = \varepsilon\varepsilon_f \cos\nu, \\ &\left(\omega_1 - \frac{\nu}{\tau}\right)(\xi_2 - \varepsilon) + \left(\omega_2 - \frac{\nu}{\tau}\right)(\xi_1 - \varepsilon) \\ &\qquad = -\varepsilon\varepsilon_f \sin\nu.\end{aligned} \tag{17}$$

Solving for $\tau, \varepsilon_f$ we obtain

$$\varepsilon_f = (\varepsilon \sin \nu)^{-1} \cdot \left[\frac{\nu}{\tau}(\xi_1 + \xi_2 - 2\varepsilon) - \omega_1(\xi_2 - \varepsilon) - \omega_2(\xi_1 - \varepsilon)\right] \quad (18)$$

and

$$[\omega_1\omega_2 + \varepsilon(\xi_1 + \xi_2) - \xi_1\xi_2 - [\omega_1(\xi_2 - \varepsilon) + \omega_2(\xi_1 - \varepsilon)]\cot \nu] \cdot \tau^2 + [(\xi_1 + \xi_2 - 2\varepsilon)\cot \nu - (\omega_1 + \omega_2)]\nu \cdot \tau + \nu^2 = 0, \quad (19)$$

what provides the borders of stability domains in a parametric form $\tau = \tau(\nu)$, $\varepsilon_f = \varepsilon_f(\nu)$.

These results are illustrated in Fig. 10(a), where we compare the control domains for the cases of perfect and imperfect measurement and stimulation. By perfect measurement/stimulation here we mean that the mean field of the whole population of $N$ elements is being registered, and that the whole population is affected by feedback signal. Correspondingly, by imperfect we denote the case when the mean field of the second population of size $N/2$ is being registered, and the first population, also of size $N/2$, is affected. The parameters used in this figure are $\xi_1 = \xi_2 = 0.02$, $\omega_1 = \omega_2 = 1$, $\varepsilon = 0.05$. We can conclude that the domains of control generally shrink and shift with respect to the case of perfect control. This is confirmed by numerical simulation for the ensemble of Rulkov neurons; this simulation also demonstrates that the maximal possible suppression factor remains nearly the same. Next, analysis of control domains provided by Eqs. (18) and (19) shows that suppression is also possible, if two populations are not identical. It can be achieved for small frequency mismatch ($\omega_1 = 1$, $\omega_2 = 1.05$), when two coupled population remain synchronized, see Fig. 10(b).

Finally, we illustrate the case when the subpopulation, where the measurement is performed, is by itself stable (in Eqs. (14) it corresponds to $\xi_2 < 0$). This situation may be considered as a model of suppression with a measurement from a surface electrode.[5] An example of control domains for parameters $\omega_1 = 1$, $\omega_2 = 1.02$, $\xi_1 = 0.02$, and $\xi_2 = -0.02$, $\varepsilon = 0.02$ are shown in Fig. 10(c).

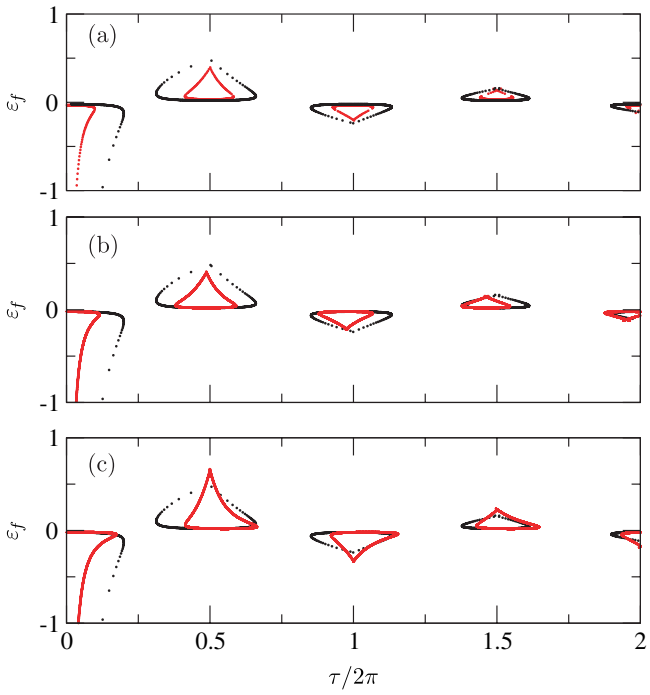


Fig. 10. Domains of control for the case of perfect (black) and imperfect (red) measurement/stimulation, for the case of identical (a) and nonidentical (b) subpopulations, see text. Panel (c) illustrates the case when the population, where the measurement is performed, is by itself stable.

## 5. Discussion

We have analyzed the efficiency of the delayed feedback control of collective rhythms in a network of neuronal oscillators as a possible tool for manipulation of the neural synchrony. We have considered different practical important factors like influence of measuremental noise, imperfection of measurement and stimulation, etc. We have created a new step towards more realistic modeling by considering population of excitatory and inhibitory neurons with synaptic connections, and we have shown that the delayed control technique works in this case as well. In summary, we have demonstrated that the technique may be useful for neurophysiological experiments, e.g. with brain slice cultures. An important feature of our approach is that it does not require any knowledge of the parameters of individual neurons or access to them. Only collective rhythms of the population should be measured, and the stimulation should act on the ensemble as an entity.

We mention also several limitations of the technique. First, it is efficient only if the system is not

[5]P. A. Tass, private communication.

too far from the bifurcation point. Next, the appropriate parameters (delay and feedback strength) can be only determined by trial and error, and there exist so far no methods to determine them *a priori*.

## Acknowledgments

We thank Nikolai Rulkov for his help and detailed comments. We have profited a lot from discussions with P. A. Tass. This work has been supported by DFG (SFB 555), IKYDA-DAAD Program, and Land Brandenburg (Promotionskolleg "Computational neuroscience").

## References

Behabid, A. L., Pollak, P., Gervason, C., Hoffmann, D., Gao, D. M., Hommel, M., Perret, J. E. & De Rougemont, J. [1991] "Long-term suppression of tremor by chronic stimulation of the ventral intermediate thalamic nucleus," *Lancet* **337**, 403–406.

Bevan, M. D., Magill, P. J., Terman, D., Bolam, J. P. & Wilson, C. J. [2002] "Move to the rhythm: Oscillations in the subthalamic nucleus-external globus pallidus network," *Trends in Neurosci.* **25**, 523–531.

Crawford, J. D. [1994] "Amplitude expansions for instabilities in populations of globally-coupled oscillators," *J. Stat. Phys.* **74**, 1047–1084.

Hindmarsh, J. L. & Rose, R. M. [1984] "A model for neuronal bursting using three coupled first order differential equations," *Proc. Roy. Soc. London Ser. B* **221**, 87.

Kuramoto, Y. [1975] "Self-entrainment of a population of coupled nonlinear oscillators," in *Int. Symp. Mathematical Problems in Theoretical Physics*, ed. Araki, H., Lecture Notes in Physics, Vol. 39 (Springer, NY), p. 420.

Kuramoto, Y. [1984] *Chemical Oscillations, Waves and Turbulence* (Springer, Berlin).

Mirollo, R. & Strogatz, S. [1990] "Synchronization of pulse-coupled biological oscillators," *SIAM J. Appl. Math.* **50**, 1645–1662.

Ozden, I., Venkataramani, S., Long, M. A., Connors, B. W. & Nurmikko, A. V. [2004] "Strong coupling of nonlinear electronic and biological oscillators: Reaching the 'amplitude death' regime," *Phys. Rev. Lett.* **93**, 158102.

Pikovsky, A. & Ruffo, S. [1999] "Finite-size effects in a population of interacting oscillators," *Phys. Rev. E* **59**, 1633–1636.

Rosenblum, M. G. & Pikovsky, A. S. [2004a] "Controlling synchrony in ensemble of globally coupled oscillators," *Phys. Rev. Lett.* **92**, 114102.

Rosenblum, M. G. & Pikovsky, A. S. [2004b] "Delayed feedback control of collective synchrony: An approach to suppression of pathological brain rhythms," *Phys. Rev. E.* **70**, 041904.

Rubin, J. & Terman, D. [2004] "High frequency stimulation of the subthalamic nucleus eliminates pathological thalamic rhythmicity in a computational model," *J. Comp. Neurosci.* **16**, 211–235.

Rulkov, N., Timofeev, I. & Bazhenov, M. [2004] "Oscillations in large-scale cortical networks: Map-based model," *J. Comp. Neurosci.* **17**, 203–222.

Rulkov, N. F. [2001] "Regularization of synchronized chaotic bursts," *Phys. Rev. Lett.* **86**, 183–186.

Rulkov, N. F. [2002] "Modeling of spiking-bursting neural behavior using two-dimensional map," *Phys. Rev. E.* **65**, 041922.

Tass, P. A. [1999] *Phase Resetting in Medicine and Biology. Stochastic Modelling and Data Analysis* (Springer-Verlag, Berlin).

Tass, P. A. [2001] "Effective desynchronization by means of double-pulse phase resetting," *Europhys. Lett.* **53**, 15–21.

Tass, P. A. [2002a] "Desynchronization of brain rhythms with soft phase-resetting techniques," *Biol. Cyber.* **87**, 102–115.

Tass, P. A. [2002b] "Effective desynchronization with a resetting pulse-train followed by a single pulse," *Europhys. Lett.* **55**, 171–177.

Tass, P. A. [2002c] "Effective desynchronization with a stimulation technique based on soft phase resetting," *Europhys. Lett.* **57**, 164–170.

Tass, P. A. [2002d] "Effective desynchronization with bipolar double-pulse stimulation," *Phys. Rev. E.* **66**, 036226.

Tass, P. A. [2003] "A model of desynchronizing deep brain stimulation with a demand-controlled coordinated reset of neural subpopulations," *Biol. Cybern.* **89**, 81–88.

van Vreeswijk, C. & Hansel, D. [2001] "Patterns of synchrony in neural networks with spike adaptation," *Neural Comput.* **13**, 959–992.

Winfree, A. T. [1980] *The Geometry of Biological Time* (Springer, Berlin).